Infrared study of oxygen vacancies in $KTaO_3$

S. Jandl, M. Banville, P. Dufour, and S. Coulombe
Centre de Recherche en Physique du Solide, Université de Sherbrooke, Sherbrooke, Québec, Canada J1K 2R1

L. A. Boatner
Solid State Division, Oak Ridge National Laboratory, Oak Ridge, Tennessee 37831
(Received 2 August 1990)

The temperature dependence of the reflectance in the range 30–1500 cm^{-1}, the transmission in the vicinity of 3500 cm^{-1}, and the Raman spectrum at 15 K of high-purity $KTaO_3$ are compared with the same properties of reduced $KTaO_3$ with oxygen vacancies. Phonons at critical points in the Brillouin zone are observed, while disruption of the Ta-O-Ta chains in the reduced material generates at all temperatures an overdamping of the ferroelectric soft mode, which is no longer detectable. The analysis of the transmittance of both samples in the vicinity of the OH stretching-mode frequency supports the conclusion that an interaction exists between the OH radicals and the ferroelectric soft mode in the high-purity $KTaO_3$ samples.

INTRODUCTION

$KTaO_3$ or potassium tantalate is designated as a quantum paraelectric or incipient ferroelectric that does not undergo a ferroelectric phase transition like $BaTiO_3$ or $KNbO_3$. Nevertheless, the $KTaO_3$ dielectric constant does increase rapidly with decreasing temperature, while its lowest infrared-active mode softens.[1–5] $KTaO_3$ is a model system in which to study soft-mode behavior[6] and phonon-phonon interactions.[7] Chaves, Barreto, and Ribeiro[8] have developed a theory for this system based upon a fourth-order anharmonic Hamiltonian, while Migoni, Biltz, and Bäuerle[9] have invoked a nonlinear anisotropic behavior of the O^{2-} polarizability. Recently, Perry *et al.*[10] showed that only the nonlinear polarization of the oxygen along the Ta-O-Ta chains can account for the observed second-order Raman scattering and frequency shift of the ferroelectric soft mode. Hybridization of $O^{2-}p$ states with neighboring Ta d states according to Bussmann *et al.*[11] would also provide an additional anisotropic enhancement of polarizability along the Ta-O-Ta chains. In addition to the strong second-order Raman scattering, spectra of pure $KTaO_3$ samples exhibit weak peaks at the position of single-phonon frequencies 200 cm^{-1} (TO_2), 550 cm^{-1} (TO_3), and 827 cm^{-1} (LO_2), resulting from microscopic ferroelectric regions extending over a few unit cells.[12–15] Grenier *et al.*[16] observed a near-infrared luminescence around 14 570 cm^{-1} associated with Ta^{3+} ions near oxygen vacancies in $KTaO_3$, and Jandl, Grenier, and Boatner[17] showed that oxygen vacancies are responsible for the formation of ferroelectric microdomains. Bäuerle *et al.*[18] investigating the ferroelectric soft mode in semiconducting $SrTiO_3$ by temperature-derivative Raman spectroscopy and inelastic neutron scattering, observed a remarkable increase of the ferroelectric mode frequency as the oxygen vacancy concentration increases due to the influence of an enhanced polarizability in the TiO_6^{2-} octahedron. One of the prominent impurities found in $KTaO_3$ is hydrogen as evidenced by the OH stretching vibration mode in the near infrared at about 3500 cm^{-1}. Houde *et al.*[19] have claimed that the splitting of the OH mode observed at low temperature is related to fluctuations of the ferroelectric soft mode. Jovanovic *et al.*,[20] however, have attributed the OH-mode sidebands to interactions with impurities and defect centers.

In the present article we study the effect of oxygen vacancies on the ferroelectric soft mode and the OH stretching vibration in $KTaO_3$ by comparing the infrared spectra of high-purity and reduced high-purity samples.

SAMPLE PREPARATION AND EXPERIMENTAL SETUP

A high-purity $KTaO_3$ crystal was cut in half. One-half of the crystal was used as the reference sample, and the other was subjected to an anneal for 2 h in a hydrogen atmosphere at 1000 K. The annealed crystal remained colorless even though it was reduced, and consequently, was slightly conducting ($N < 10^{18}$ cm^{-3}).[21] The two samples were mounted in a continuous flow, regulated-temperature helium cryostat, and infrared reflectance and transmittance spectra were taken with a Fourier-transform interferometer (BOMEN DA3.002) using globar and mercury sources, Ge and Si bolometers, and KBr and Mylar beamsplitters. The reflectance spectra in the range from 4500 to 30 cm^{-1} were normalized with respect to aluminum spectra taken at the specimen temperature. Reflectance spectra of high-purity and reduced high-purity $KTaO_3$ in the range of 1500 to 30 cm^{-1} and the transmittance around 3495 cm^{-1} are shown in Figs. 1 and 2, respectively, as a function of temperature.

ANALYSIS OF THE REFLECTANCE SPECTRA AND DISCUSSION

The high-frequency dielectric function $\epsilon(\infty)$, the transverse and longitudinal frequencies ω_{jT} and ω_{jL}, and the

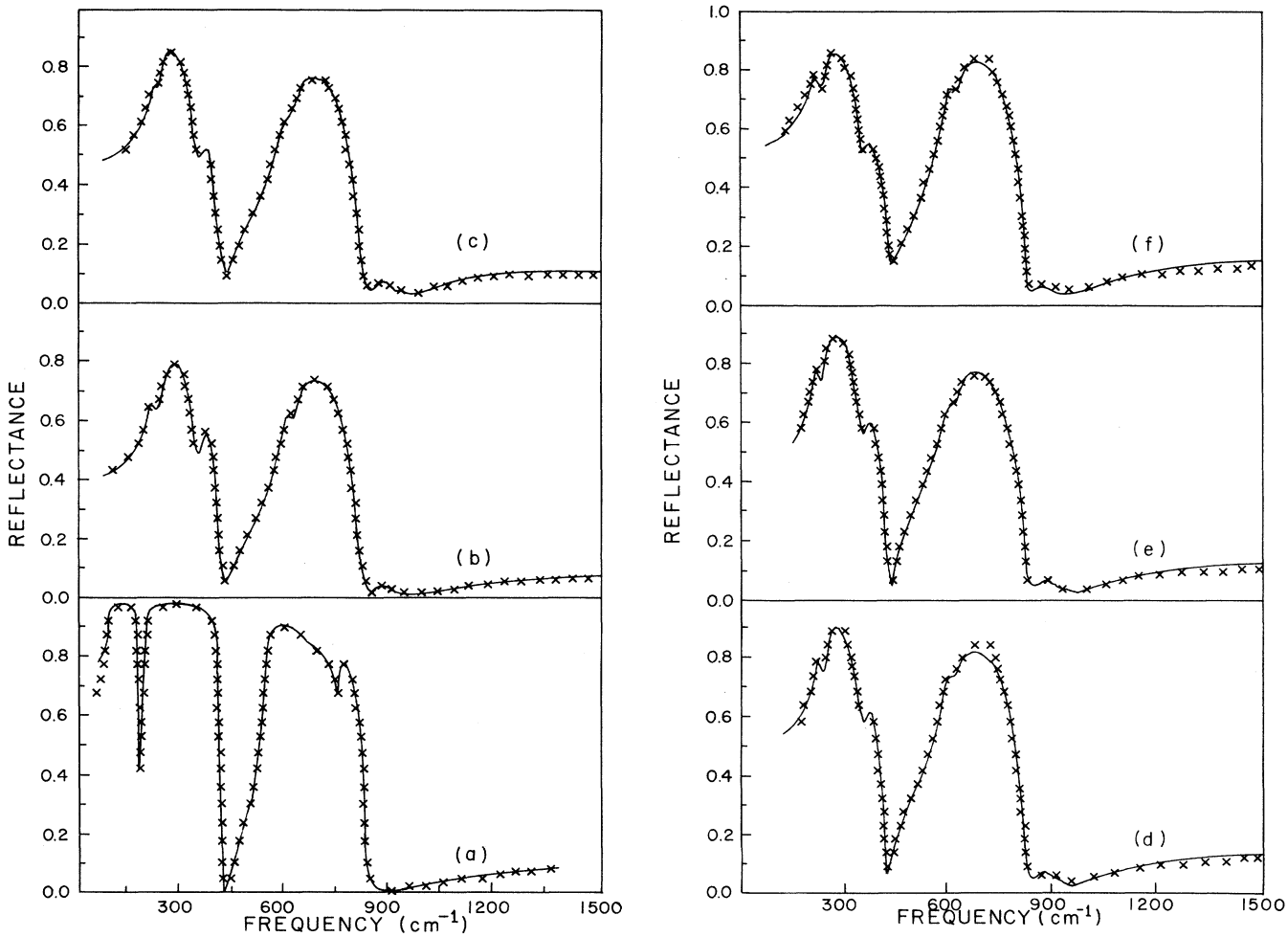

FIG. 1. Reflectance spectra of (a) ultrapure $KTaO_3$ at 300 K and reduced $KTaO_a$ at (b) 300 K, (c) 200 K, (d) 100 K, (e) 50 K, and (f) 10 K. × are the experimental data and the solid line is the model fit.

damping factor of the phonons γ_j were obtained by fitting the factorized dielectric function given in Eq. (1) to the observed spectra:[22]

$$\epsilon(\omega)=\epsilon(\infty)\prod_{j=1}^{M}\frac{\omega_{jL}^2-\omega^2-i\gamma_j\omega}{\omega_{jT}^2-\omega^2-i\gamma_j\omega}\ . \tag{1}$$

Such an expression is necessary to describe adequately a system having a weak mode whose transverse frequency falls between the transverse and longitudinal frequencies of a stronger mode. In such a case, the weaker mode will be described by a longitudinal frequency which is smaller than its transverse frequency. The longitudinal frequencies ω_{jL} in Eq. (1) are the frequencies Ω_{jL} of the isolated modes shifted because of their overlap with other modes. The isolated-mode longitudinal frequency is calculated from the relation

$$\Omega_{kL}=\omega_{kT}\left[\frac{S_k}{\epsilon_k}+1\right]^{1/2}, \tag{2}$$

where ϵ_k is the local dielectric constant obtained from

$$\epsilon_k=\epsilon(\infty)+\sum_{j=k+1}^{M}S_j\ , \tag{3}$$

where the oscillators are ordered with increasing transverse frequency, and S_k the oscillator strength is calculated from a generalized Lyddane-Sachs-Teller relation

$$S_k=\epsilon(\infty)\left[\left[\frac{\omega_{kL}}{\omega_{kT}}\right]^2-1\right]\prod_{m\neq k}\frac{\omega_{mL}^2-\omega_{kT}^2}{\omega_{mT}^2-\omega_{kT}^2}\ . \tag{4}$$

The high-purity $KTaO_3$ infrared reflectance and the associated fit at room temperature are shown in Fig. 1(a). The set of parameters given in Table I were obtained by minimization of the X^2 function between the reflectivity predicted by the model (1) and the data by variation of the parameters. The transverse frequencies correspond to previously published values,[1–5] while the longitudinal frequencies and the damping and strength parameters are more explicitly calculated with the factorized oscillator model and the corresponding Eqs. (2)–(4). While the first three phonons (ω_T=98, 201, and 548 cm^{-1}) have a small damping and a significant oscillator strength (especially

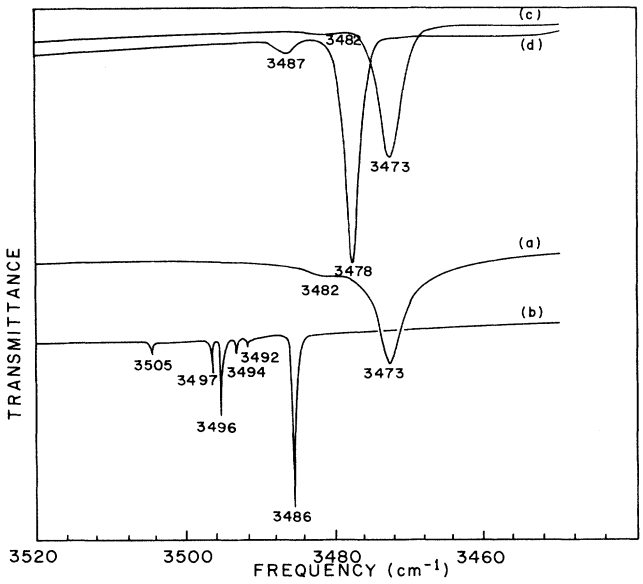

FIG. 2. Infrared transmittance of ultrapure $KTaO_3$ at (a) 300 K, (b) 15 K and reduced $KTaO_3$ at (c) 300 K, (d) 15 K.

for the ferroelectric soft mode), the oscillators at 710 and 752 cm^{-1} correspond to combination bands with a weak oscillator strength and a strong damping.

In Figs. 1(b)–1(f), the infrared spectra of the reduced high-purity $KTaO_3$ are shown with the model fit as a function of temperature. In Table II the corresponding parameters used in the fit are given for each temperature. All transverse frequencies ω_T of the reduced sample with oxygen vacancies differ from those of the high-purity specimen. Actually, the infrared active modes of high-purity $KTaO_3$ are no longer observed. The ω_T frequencies listed in Table II correspond to vibrations detected in stress-induced Raman,[23] differential Raman, differential fluorescence measurements,[24] and vibronic spectra of pure $KTaO_3$.[16] The 212- and 593-cm^{-1} modes are phonons at the [100] zone boundary.[24–26] The 256-cm^{-1} mode, observed only in differential fluorescence, is attributed to a critical point.[24] The 364-cm^{-1} mode is a combination of the two phonons (191 and 172 cm^{-1}) at the [100] zone boundary,[23,24] while the 427- and 631-cm^{-1} features correspond to local modes observed in the vibronic spectra.[16] Finally the 882- and 948-cm^{-1} vibrations are, respectively, combinations of 631 with 256 cm^{-1} and 593 with 364 cm^{-1}.

TABLE I. Phonon oscillator parameters of ultrapure $KTaO_3$ at 300 K. All frequencies and dampings are in cm^{-1}.

ω_T	ω_L	γ	S	Ω_L
91	423	6.5	172.	335
201	186	6	6.7	282
548	821	13	2.2	667
710	701	130	0.06	715
752	750	20	0.01	753

$\epsilon(\infty)=4.6$ $X^2=.0011$

The ω_T frequencies in the reduced $KTaO_3$ show a tendency toward softening at low temperatures, while the oscillator strengths and their corresponding longitudinal frequency Ω_L (Ref. 2) increase. Such a behavior would result from an ordering of the ferroelectric microdomains observed in photoluminescence.[16,17] The phonon damping in the reduced $KTaO_3$ is typically 3 times larger, reflecting the effects associated with the oxygen vacancies. Even though the overall infrared reflectance is strongly affected by disorder-induced phonons, the second-order Raman scattering of the reduced $KTaO_3$ sample is almost identical to that of the untreated high-purity sample (Fig. 3). The two new peaks indicated by arrows observed at 200 and 548 cm^{-1} are due to symmetry breaking in microdomains of oxygen vacancies. They correspond, respectively, to TO_2 and TO_3 of the infrared-active modes of pure $KTaO_3$. The major effect produced by the oxygen vacancies is thus seen to be a breakdown of the momentum conservation rule without any noticeable variation of the phonon frequencies.

Another important consequence of the oxygen vacancies is the disappearance in the infrared reflectance spectra of the ferroelectric soft mode at all temperatures probably because of overdamping by partial disturbances in the Ta-O-Ta chains. Consequently, it becomes ambiguous to interpret single lines in temperature-derivative second-order Raman of reduced $SrTiO_3$ as observable overtones of a ferroelectric mode that is strongly shifted toward higher frequencies.[18] The disappearance of the ferroelectric soft mode in the reduced sample reflects the important role played by the oxygen polarizability, the Ta-O-Ta chains, and the long-range interactions. These interactions are less important in the second-order Ra-

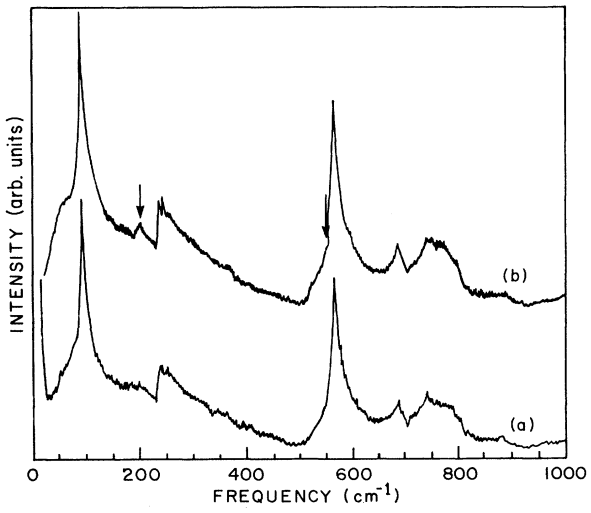

FIG. 3. Raman scattering of (a) ultrapure $KTaO_3$ and (b) reduced $KTaO_3$.

TABLE II. Phonon oscillator parameters of reduced $KTaO_3$ at various temperatures. All frequencies and dampings are in cm^{-1}.

T	ω_T	ω_L	γ	S	Ω_L
300	215	429	25	4.5	245
200	221	431	20	6.9	254
100	223	427	15	10.1	266
50	220	426	13	6.8	250
10	214	428	32	21.6	313
300	256	226	40	8.0	373
200	250	230	30	10.7	358
100	250	233	20	12.3	356
50	249	228	25	13.2	370
10	246	235	24	7.2	313
300	593	816	45	1.9	705
200	598	819	46	2.3	689
100	590	820	40	4.0	742
50	594	821	48	3.2	722
10	592	817	39	3.6	726
300	364	342	50	0.6	380
200	369	343	55	0.8	385
100	367	345	60	0.9	382
50	369	346	56	0.8	383
10	366	346	51	0.8	380
300	427	412	31	0.01	427
200	425	406	32	0.09	427
100	421	405	35	0.08	423
50	419	405	33	0.09	420
10	419	406	38	0.10	421
300	631	621	48	0.5	671
200	628	617	45	1.2	691
100	627	624	30	0.4	645
50	629	622	37	0.7	663
10	629	624	33	0.5	652
300	882	898	53	0.04	886
200	881	898	50	0.06	885
100	876	896	70	0.07	880
50	878	899	80	0.07	883
10	874	899	80	0.08	879
300	948	952	47	0.01	949
200	937	944	45	0.02	939
100	927	937	60	0.03	929
50	933	940	60	0.02	934
10	935	937	57	0.01	935

T	$\epsilon(\infty)$	X^2
300	4.0	0.000 17
200	5.8	0.000 38
100	6.5	0.000 91
50	6.0	0.000 80
10	6.6	0.000 52

man processes as can be seen from the similarity of the untreated high-purity and the reduced high-purity sample spectra.

STUDY OF THE OH STRETCHING MODE

Hydrogen impurities in $KTaO_3$ and $SrTiO_3$ have been the subject of a number of recent investigations.[19,20,27–29] Two origins have been proposed for the OH-stretching-mode sidebands observed at low temperatures. Impurities have been invoked by some authors,[20,28] while others have related the low-temperature splitting to fluctuations of the ferroelectric soft mode.[19,29] Our reduced $KTaO_3$ sample with its overdamped ferroelectric mode constitutes a test for either explanation. We have measured the high-resolution (~ 0.05 cm^{-1}) transmission spectra in the vicinity of the OH stretching mode ~ 3480 cm^{-1}. Figure 2 shows the transmission of the untreated high-purity sample [Figs. 2(a) and 2(b)] and the reduced sample [Figs. 2(c) and 2(d)] for both temperatures 300 and 15 K. At 300 K both samples have identical absorption bands located at 3473 and 3482 cm^{-1} with comparable half-bandwidths (HBW ~ 3 cm^{-1}), suggesting that there is no effect from the oxygen vacancies on the OH stretching mode. However, a large difference is observed at 15 K. While six narrow bands (HBW ~ 0.3 cm^{-1}) develop in the untreated high-purity sample at the same frequencies reported previously,[19] the two bands of the reduced high-purity sample are shifted to slightly lower frequencies with no multiple side bands, and their HBW remains large (~ 2.6 cm^{-1}) because of disorder induced by the oxygen vacancies. At high temperature two bands occur at the same frequencies (3473 and 3482 cm^{-1}) in both samples. They are interpreted as originating from the inequivalent positions of the OH dipoles due to the presence of impurities in the sample. However, at low temperature there is a significant frequency shift between the two bands at 3478 and 3487 cm^{-1} of the reduced sample versus the corresponding bands at 3486 and 3496 cm^{-1} for the untreated high-purity sample. Identical impurities, even in small concentrations, should be present equally in both samples since they were cut originally from the same high-purity crystal. If impurities were the dominant influence on the OH stretching-mode, their effect should be the same for the two samples both at high and low temperatures. In the high-purity sample the observation of six narrow bands confirms the predicted location of the hydrogen atoms in the neighborhood of an oxygen atom along the K-O diagonal.[19] When the atomic displacements associated with the zone-center ferroelectric phonon are taken into account, three inequivalent positions for each band of the OH dipole occur. Hence the difference between the two absorption spectra [Figs. 2(b) and 2(d)] is due to the presence of the ferroelectric soft mode in the high-purity sample and its absence in the treated sample.

CONCLUSION

In $KTaO_3$ with oxygen vacancies, the infrared reflectance is strongly perturbed, while the Raman spectrum is only slightly influenced. The ferroelectric soft mode is strongly overdamped because of induced disorder in the Ta-O-Ta chains, and consequently the OH stretching-mode frequencies are affected, pointing to the existence of an interaction between the OH radicals and ferroelectric fluctuations in pure $KTaO_3$.

ACKNOWLEDGMENTS

This work is supported by grants from the Natural Sciences and Engineering Research Council of Canada and the Fonds pour la formation de chercheurs et l' aide à la recherche (Québec).

[1]G. Rupprecht and R. O. Bell, Phys. Rev. **135**, A748 (1964).
[2]R. C. Miller and W. G. Spitzer, Phys. Rev. **129**, 94 (1963).
[3]A. S. Barker, Phys. Rev. **145**, 391 (1966).
[4]C. H. Perry and T. F. McNelly, Phys. Rev. **154**, 456 (1967); C. H. Perry and N. E. Tornberg, *ibid.* **183**, 595 (1969).
[5]K. F. Pai, T. J. Parker, N. E. Tornberg, R. P. Lowndes, and W. G. Chambers, Infrared Phys. **18**, 327 (1978); K. F. Pai, T. J. Parker, and R. P. Lowndes, Ferroelectrics **21**, 337 (1978).
[6]J. F. Scott, Rev. Mod. Phys. **46**, 83 (1974).
[7]A. S. Barker, Jr. and J. J. Hopfield, Phys. Rev. **135**, A1721 (1964).
[8]A. S. Chaves, F. C. S. Barreto, and L. A. A. Ribeiro, Phys. Rev. Lett. **37**, 618 (1976).
[9]R. Migoni, H. Biltz, and D. Bäuerle, Phys. Rev. Lett **37**, 1155 (1976).
[10]C. H. Perry, R. Currat, H. Buhay, R. M. Migoni, W. G. Stirling, and J. D. Axe, Phys. Rev. B. **39**, 8666 (1989).
[11]A. Bussmann, H. Biltz, R. Rouspiess, and K. Schwarz, Ferroelectrics **25**, 343 (1980).
[12]Y. Yacoby, Phys. Rev. B **31**, 275 (1978).
[13]R. L. Prater, L. L. Chase, and L. A. Boatner, Phys. Rev. B. **23**, 221 (1981).
[14]B. Salce, A. M. De Goer, and L. A. Boatner, J. Phys. (Paris) Colloq. **42**, C-6424 (1981).
[15]H. Uwe, K. B. Lyons, H. L. Carter, and P. A. Fleury, Phys. Rev. B **33**, 6436 (1986).
[16]P. Grenier, G. Bernier, S. Jandl, B. Salce, and L. A. Boatner, J. Phys. **1**, 2515 (1989).
[17]S. Jandl, P. Grenier, and L. A. Boatner, Ferroelectrics **107**, 73 (1990).
[18]D. Bäuerle, D. Wagner, M. Wöhlecke, B. Borner, and H. Kraxenberger, Z. Phys. B **38**, 335 (1980); A. Bussmann-Holder, H. Bilz, D. Bäuerle, and D. Wagner, Z. Phys. B **41**, 353 (1981).
[19]D. Houde, S. Jandl, P. Grenier, C. Pépin, and Y. Lépine, Ferroelectrics **77**, 55 (1988).
[20]A. Jovanovic, M. Wöhlecke, S. Kapphan, and B. Hellermann, Ferroelectrics **107**, 85 (1990).
[21]S. H. Wemple, Phys. Rev. **137**, 1575 (1965).
[22]D. H. Berremann and F. C. Unterwald, Phys. Rev. B **15**, 2316 (1977).
[23]H. Uwe and T. Sakudo, Phys. Rev. B **15**, 337 (1977).

[24]Y. Yacoby and A. Linz, Phys. Rev. B **9**, 2723 (1974).
[25]W. G. Nilsen and J. G. Skinner, J. Chem. Phys. **47**, 1413 (1967).
[26]C. H. Perry, J. H. Fertel, and T. F. McNelly, J. Chem. Phys. **47**, 1619 (1967).
[27]G. Weber, S. Kapphan, and M. Wöhlecke, Phys. Rev. B **34**, 8406 (1986).
[28]R. Waser, Z. Naturforsch. A **42**, 1357 (1987).
[29]D. Houde, Y Lépine, C. Pépin, S. Jandl, and J. L. Brebner, Phys. Rev. B **35**, 4948 (1987).